APL Materials

Temperature dependence of the Seebeck coefficient of epitaxial β-Ga_2O_3 thin films

Cite as: APL Mater. **7**, 022526 (2019); https://doi.org/10.1063/1.5084791
Submitted: 07 December 2018 • Accepted: 14 January 2019 • Published Online: 07 February 2019

Johannes Boy, Martin Handwerg, Robin Ahrling, et al.

COLLECTIONS

Paper published as part of the special topic on Wide Bandgap Oxides

ARTICLES YOU MAY BE INTERESTED IN

A review of Ga_2O_3 materials, processing, and devices
Applied Physics Reviews **5**, 011301 (2018); https://doi.org/10.1063/1.5006941

Data analysis for Seebeck coefficient measurements
Review of Scientific Instruments **84**, 065102 (2013); https://doi.org/10.1063/1.4807697

MOCVD grown epitaxial β-Ga_2O_3 thin film with an electron mobility of 176 cm^2/V s at room temperature
APL Materials **7**, 022506 (2019); https://doi.org/10.1063/1.5058059

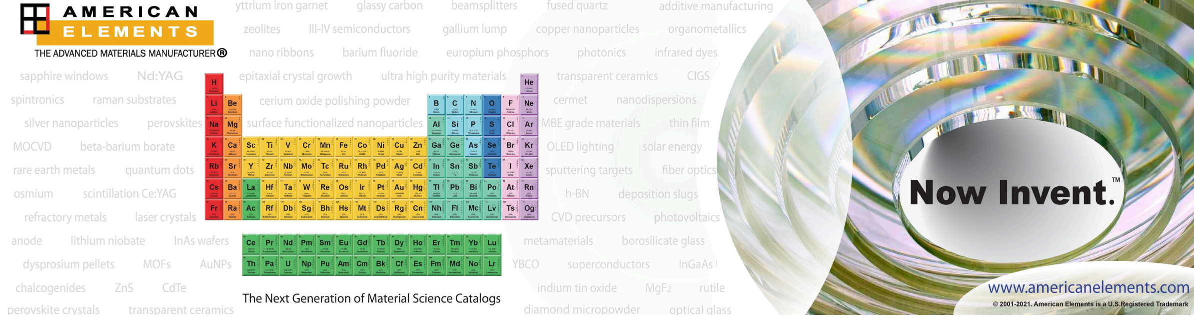

© 2019 Author(s).

Temperature dependence of the Seebeck coefficient of epitaxial β-Ga_2O_3 thin films

Cite as: APL Mater. 7, 022526 (2019); doi: 10.1063/1.5084791
Submitted: 7 December 2018 • Accepted: 14 January 2019 •
Published Online: 7 February 2019

Johannes Boy,[1,a)] Martin Handwerg,[1] Robin Ahrling,[1] Rüdiger Mitdank,[1] Günter Wagner,[2] Zbigniew Galazka,[2] and Saskia F. Fischer[1]

AFFILIATIONS

[1]Novel Materials Group, Humboldt-Universität zu Berlin, Newtonstraße 15, 12489 Berlin, Germany
[2]Leibniz-Institut für Kristallzüchtung, Max-Born-Strasse 2, 12489 Berlin, Germany

[a)]boy@physik.hu-berlin.de

ABSTRACT

The temperature dependence of the Seebeck coefficient of homoepitaxial metal organic vapor phase grown, silicon doped β-Ga_2O_3 thin films was measured relative to aluminum. For room temperature, we found the relative Seebeck coefficient of $S_{\beta\text{-}Ga_2O_3\text{-}Al} = (-300\pm20)\,\mu V/K$. At high bath temperatures T > 240 K, the scattering is determined by electron-phonon-interaction. At lower bath temperatures between T = 100 K and T = 300 K, an increase in the magnitude of the Seebeck coefficient is explained in the frame of Stratton's formula. The influence of different scattering mechanisms on the magnitude of the Seebeck coefficient is discussed and compared with Hall measurement results.

© 2019 Author(s). *All article content, except where otherwise noted, is licensed under a Creative Commons Attribution* (CC BY) *license* (*http://creativecommons.org/licenses/by/4.0/*). https://doi.org/10.1063/1.5084791

In the past years, β-Ga_2O_3 crystals and thin films have proved to be promising materials for high power devices.[1–5] Therefore heat transport mechanisms are of great interest. The energy dissipation sums up by Peltier, Fourier, and Joule heating terms, which are a function of the Seebeck coefficient S, the electrical conductivity σ, and the thermal conductivity λ, respectively. While the temperature dependent electrical[6,7] and thermal properties[8,9] are known and understood, the thermoelectric parameters remain to be investigated. For this purpose, values of the Seebeck coefficient of β-Ga_2O_3 must be known.

β-Ga_2O_3 is a transparent material, with a high bandgap E_g = 4.7 – 4.9 eV at room temperature.[10–14] The majority charge carrier type is n-type, and the effective mass has been experimentally determined to be in the order of m^* = 0.25 – 0.28 free electron masses.[14–16] β-Ga_2O_3 has been intensively studied in terms of charge carrier transport with a maximum mobility so far being μ = 153 cm^2/Vs[17] at room temperature.

In this work, we implement a microlab, based on metallic lines on the homoepitaxial metal organic vapor phase (MOVPE) grown (100) silicon doped β-Ga_2O_3 thin films, and perform temperature-dependent Seebeck measurements between T = 100 K and T = 300 K. We compare the results with calculated room temperature Seebeck coefficients based on Hall charge carrier density by using Stratton's formula.[18]

The thin films have been grown on substrates prepared from Mg-doped, electrically insulating bulk β-Ga_2O_3 single crystals, which were grown along the [010]-direction by the Czochralski method.[17,19] The substrates with (100)-orientation have been cut with a 6° off-orientation to reduce island growth[19,20] and increase the structural quality of the thin films. The MOVPE process used triethylgallium and pure oxygen as precursors. Silicon doping has been realized by tetraethyl orthosilicate. The substrate temperature was between 750 °C and 850 °C and the chamber pressure was between 5 and 100 mbar during growth.[21]

The material parameters of the samples are listed in Table I. Both β-Ga_2O_3 thin films have the same magnitude of charge carrier densities but a rather big difference in mobility. The thin films have been investigated with AFM measurements, which exhibit step-flow growth for the high mobility sample and two-dimensional island growth for the low mobility sample. This causes a low and rather high density of twin

TABLE I. Thin film thickness d, charge carrier density n, and mobility μ for the investigated β-Ga_2O_3 thin film samples at room temperature and 100 K. We have obtained doping densities in the range of $N_D = 2.1 \times 10^{18}$ cm^{-3} and $N_D = 2.2 \times 10^{18}$ cm^{-3} for the high and low mobility samples, respectively, by fits of the temperature dependent charge carrier densities. The significant difference in mobility can be explained by an enhanced density of twin boundaries in sample 2 which was previously analyzed with electron microscopy.[22] Twin boundary-electron scattering decreases the mobility over the entire temperature range.

β-Ga_2O_3 thin film	Sample 1 High mobility	Sample 2 Low mobility
d (nm)	185	212
n(T = 300 K) (cm^{-3})	(5.5 ± 0.1) × 10^{17}	(6.2 ± 0.1) × 10^{17}
μ(T = 300 K) (cm^2/V s)	103 ± 1	29 ± 1
n(T = 100 K) (cm^{-3})	(1.6 ± 0.1) × 10^{17}	(2.1 ± 0.1) × 10^{17}
μ(T = 100 K) (cm^2/V s)	233 ± 1	48 ± 1

boundaries in the high and low mobility samples, respectively. The sample growth and structural analysis was previously described in detail in the literature,[21,23] and the influence of twin boundaries was discussed by Fiedler *et al.*[22] and Ahrling *et al.*[6]

The microlabs have been manufactured by standard photolithography and magnetron sputtering of titanium (7 nm) and gold (35 nm) after cleaning with acetone and isopropanol and subsequent drying. The metal lines of the microlab are isolated due to a Schottky contact relative to the β-Ga_2O_3 thin film. Ohmic contacts with the β-Ga_2O_3 thin film were achieved by direct wedge bonding with an Al/Si-wire (99%/1%) on the deposited metal structure,[6] creating point contacts. To keep some parts of the microlab isolated relative to the thin film, the electrical contacts were prepared by attaching gold wire with indium to the Ti/Au metal lines.

Figure 1 shows the microlab, which allows the measurement of the Seebeck coefficient, charge carrier density, and conductivity.

Figure 1(a) displays a scheme of the microlab. It consists of a two-point line heater at the top, where an electrical current is imprinted to create Joule heating, resulting in a temperature difference ΔT across the sample. Two four-point metal lines close to (hot) and far from (cold) the heater line serve as thermometers. The temperature dependent measurement of their resistances follows the Bloch-Grüneisen law[24] and can be used to calculate the temperature difference in the area of the four-point resistances.

For the determination of the Seebeck coefficient, the exact temperature difference between the contacts must be known. Therefore, the Al-β-Ga_2O_3 Ohmic contacts were localized directly on the thermometers at positions I and II (see the supplementary material).

The experimental procedure involves measurement of the thermovoltage for as long as it takes to stabilize the temperature difference across the sample. Afterwards, the four-point resistances of the thermometers are measured. This procedure is repeated for several heating currents before the bath temperature is changed in intervals of 10 K.

Figure 1(b) illustrates a cross-sectional view of the samples. The Mg-doped electrically insulating β-Ga_2O_3 substrate

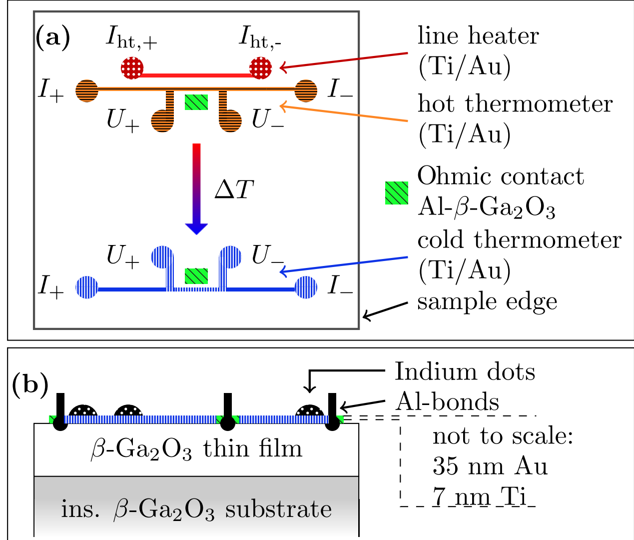

FIG. 1. (a) gives a schematic overview of the function of the Seebeck microlab. A two point conductor at the top of the scheme (red with white dots) serves as a line heater to create a temperature difference ΔT across the sample. The temperature difference is being measured by the change in the four point resistance in the thermometer lines at the bottom of the scheme (cold thermometer, blue with white vertical lines) and below the line heater (hot thermometer, orange with horizontal black lines). The little squares (green with diagonal black lines) mark the Ohmic contacts, which are used to measure the thermovoltage (U_{th}). (b) illustrates the cross section of the samples; see the text for details.

has been used to grow the Si-doped β-Ga_2O_3 thin film on top thereof. The Ti/Au metal lines of the microlab have then been deposited on the surface of the thin film, and electrical contacts have been prepared either by wedge-bonding with Al-wire (Ohmic contact) or attachment of Au-wire with indium (Schottky contact).

To ensure that the experimental setup has no influence on the Seebeck measurements, different measurement configurations have been developed. Details of the two contact configurations investigated are described in the supplementary material.

The thermovoltage U_{th} was measured as a function of temperature difference ΔT for several bath temperatures and β-Ga_2O_3 thin films.

In the right graph of Fig. 2(a), the measurements of the thermovoltage as a function of time for different temperature differences can be seen. The measurements are performed for 180 s, and the last 10% of the measured data (marked by the vertical dashed line) are used to evaluate the thermovoltage as a function of temperature difference (left graph). Due to the weaker thermal conductivity and diffusivity of β-Ga_2O_3 at higher temperatures,[8,9] it takes longer to evolve a stable temperature difference and thermovoltage as compared to lower temperatures.

The left graph of Fig. 2(a) shows the thermovoltage as a function of the temperature difference. These data can be well fitted with a linear equation, where the slope equals the

© Author(s) 2019

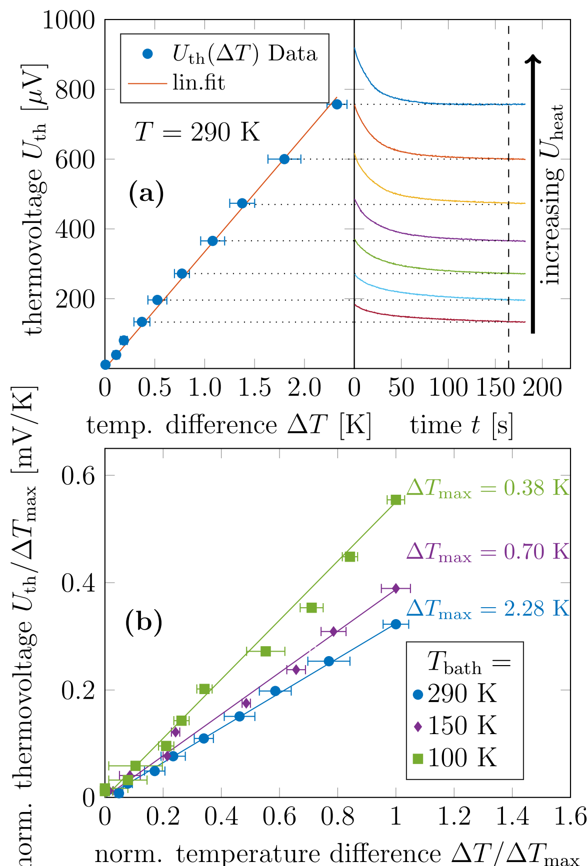

FIG. 2. (a) The thermovoltage as a function of time (right hand side) and temperature difference (left hand side) for the 185 nm thick MOVPE β-Ga_2O_3 thin film with high mobility for a bath temperature of 290 K is shown. The measurement of the thermovoltage has been performed for 180 s after applying a heating voltage to the line heater. Only the last 10% of the measured data (marked by the vertical dashed line) have been used for the evaluation to make sure a stable temperature difference has evolved. The left graph shows the average of the thermovoltage U_{th} as a function of the temperature difference ΔT between the hot and the cold thermometer. The dotted lines are a guidance for the eye. A linear fit $U_{th} = -S \cdot \Delta T + U_{off}$ has been applied to determine the Seebeck coefficient S. (b) The measured thermovoltage U_{th} normalized by the maximum of the temperature difference for the same sample has been plotted as a function of the normalized temperature difference. An offset $U_{os} < 50\ \mu$V has been subtracted from the plotted data. The corresponding bath temperatures are from bottom to top: 290 K, 150 K, and 100 K.

Seebeck coefficient

$$S = -\frac{U_{th}}{\Delta T}. \tag{1}$$

Figure 2(b) shows the normalized thermovoltage as a function of normalized temperature difference for bath temperatures of 290 K, 150 K, and 100 K with subtracted offsets for the same sample as Fig. 2(a). The change of the Seebeck coefficient as a function of bath temperature can be observed by the change in the slope of the linear fits.

Figure 3(a) displays the measured Seebeck coefficients of different β-Ga_2O_3 thin films as a function of inverse bath temperature between 100 K and 300 K. The Seebeck coefficients

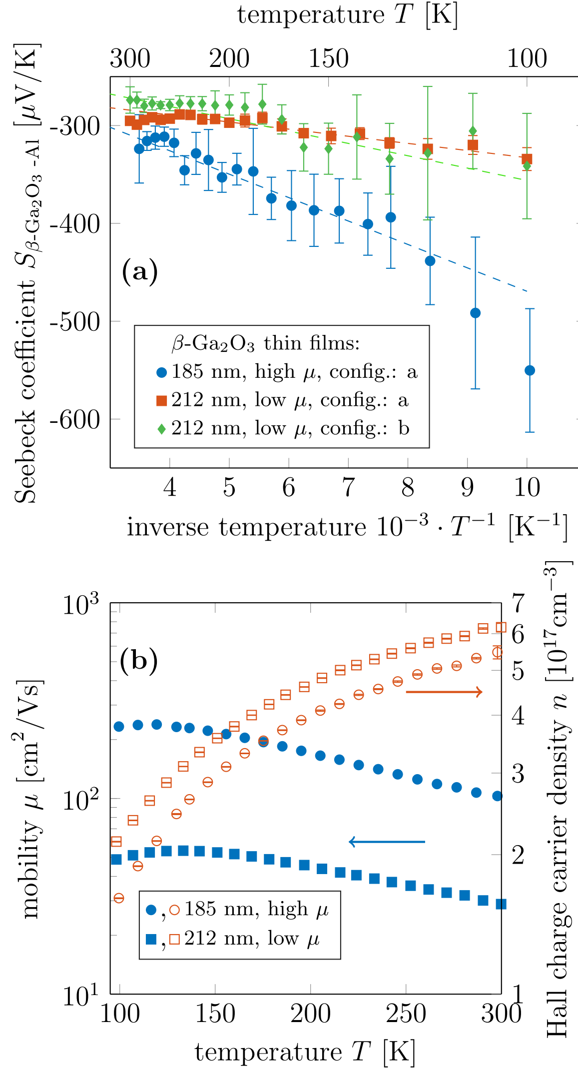

FIG. 3. (a) Seebeck coefficient S as a function of the inverse temperature T^{-1} for the investigated 185 nm thick high mobility sample 1a (blue circles) and 212 nm low mobility samples 2a (red squares) and 2b (green diamonds) relative to aluminum. A linear fit has been performed for temperatures above 130 K to investigate the Stratton formula $S = -\frac{k_B}{e}\left(r + \frac{5}{2} - \frac{E_F - E_C}{k_B T}\right)$ for constant E_F and r. (b) Mobility μ (filled symbols) and Hall charge carrier density (open symbols) n as a function of temperature T for the investigated 185 nm thick high mobility sample 1a (circles) and 212 nm low mobility samples 2a and 2b (squares).

are in the range of $S = -280\ \mu$V/K to $S = -500\ \mu$V/K above 100 K. At room temperature, the Seebeck coefficients are $S = -(300 \pm 20)\ \mu$V/K for all investigated β-Ga_2O_3 samples. The precision of the Seebeck coefficient is mainly determined by the certainty of the measurement of the temperature difference. The correction of the Seebeck coefficient due to the thermovoltage of the aluminum wire is less than 1% and does not need to be considered since it is smaller than the uncertainty of the measurement result. The high mobility β-Ga_2O_3 thin film shows a stronger increase in the Seebeck coefficient

© Author(s) 2019

for lower temperatures than the low mobility β-Ga_2O_3 thin films. We find that the investigated measurement configuration has no detectable influence on the Seebeck coefficient. The lower magnitude of the Seebeck coefficient for the 212 nm thick low mobility sample at low temperatures is expected to be due to different charge carrier scattering mechanisms.

These results are similar to those of other transparent conducting oxides like ZnO or In_2O_3, where Seebeck coefficients S in the range from S = −20 μV/K to S = −500 μV/K have been measured.[25,26]

Figure 3(b) shows the mobility μ and Hall charge carrier density n as a function of temperature T for the investigated samples. The Hall charge carrier density is similar for all samples over the entire temperature range. The plot of the mobility shows electron-phonon (EP) interaction to be the dominant scattering mechanism for T > 250 K for all samples. For lower temperatures, a transition of the dominant scattering mechanism can be observed. For T < 120 K, electron scattering with ionized impurities becomes dominant. We explain the drop of mobility over the entire temperature range for the low mobility sample by increased scattering on twin boundaries, which has previously been reported.[6,22]

The study of the temperature dependent Seebeck coefficient for β-Ga_2O_3 thin films gives an insight into the scattering mechanisms within the material.[27–29] Here we discuss the obtained Seebeck coefficients and their description by the Stratton formula,[18]

$$S_{th} = -\frac{k_B}{e}\left(r + \frac{5}{2} + \eta\right), \tag{2}$$

with the elemental charge e, the scattering parameter r, the reduced electron chemical potential $\eta = (E_C - E_F)/(k_B T)$ and the conduction band energy E_C, the Fermi energy E_F, and the Boltzmann constant k_B. The scattering parameter is related to the scattering mechanisms within the sample. In the relaxation time approximation, the scattering time and mobility are related to energy by $\tau \propto E^r$ and $\mu \propto E^r$, respectively. A first approximation of formula (2) has been plotted in Fig. 3. A linear fit with constant $r = 0.3 \pm 0.2$ and $E_C - E_F$ has been performed for T > 130 K and plotted in Fig. 3 (dashed lines). For the 185 nm thick high mobility sample, $E_C - E_F \approx 24$ meV and for the 212 nm thick low mobility samples $E_C - E_F \approx 13$ meV have been obtained. These different electron chemical potentials $E_C - E_F$ explain the different temperature dependencies but only give a rough estimation since $r = r(T)$ and $E_F = E_F(T)$.

To calculate theoretical values for the Seebeck coefficient at room temperature, we use the analytical expression after Nilsson,[30] which interpolates the range between non-degenerated and degenerated semiconductors. The reduced electron chemical potential η is then given by

$$\eta = \frac{\ln \frac{n}{N_C}}{1 - \left(\frac{n}{N_C}\right)^2} + \nu\left(1 - \frac{1}{1 + (0.24 + 1.08\nu)^2}\right), \tag{3}$$

$$\nu = \left(\frac{3\sqrt{\pi}\frac{n}{N_C}}{4}\right)^{2/3}, \tag{4}$$

with N_C being the effective density in the conduction band,

$$N_C = 2\left(\frac{2\pi m^* k_B T}{h^2}\right)^{3/2}. \tag{5}$$

With an effective mass of $m^* = (0.23 \pm 0.02) \cdot m_e$, which we obtained by fitting the measured temperature dependent charge carrier density with the neutrality equation, and a Seebeck scattering parameter of $r = -1/2$,[29,31,32] which applies for electron-phonon scattering, we calculated theoretical values using the Stratton formula (2). This calculation yields a value of $S_{th}(T > 250\ K) = (-300 \pm 20)\ \mu V/K$.

The measurement of the Seebeck coefficient and charge carrier density allows a calculation of the scattering parameter r if the effective mass m^* is known. One has to consider that the measurement of the charge carrier density using Hall measurements is influenced by the scattering of the free electrical charges as well. This is usually described by the Hall scattering factor r_H,[32] if the relaxation time τ can be expressed by $\tau \propto E^r$,

$$r_H = \Gamma(5/2 - 2r) \cdot \Gamma(5/2)/(\Gamma(5/2 - r))^2 = \mu_H/\mu, \tag{6}$$

with $\Gamma(x)$ being the gamma function, μ_H being the Hall mobility, and μ being the drift mobility. In order to correctly calculate the general scattering parameter r, one needs to know the Hall scattering parameter r_H or vice versa. Commonly for electron phonon (EP) scattering, $r_H = 1.18$ and for ionized impurity (II) scattering $r_H = 1.93$ are assumed.[32] This allows a calculation of the scattering parameter r, if we assume that only II or EP scattering dominates the charge transport. Figure 4 shows the calculated r as a function of bath temperature. The calculations were performed with Eq. (2) considering the measured Seebeck coefficients and measured charge

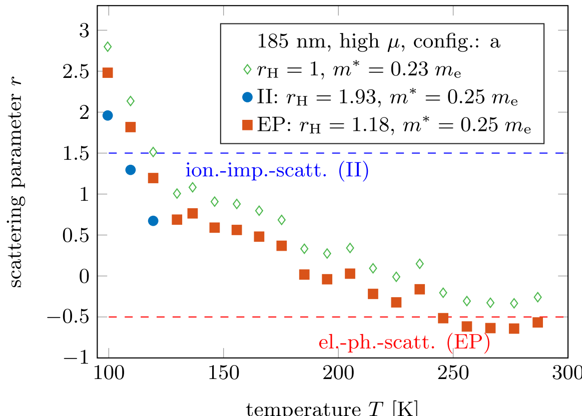

FIG. 4. Temperature dependent scattering parameters considering the measured Seebeck coefficients and measured charge carrier density for the investigated 185 nm thick high mobility sample. Various effective masses m^* and Hall scattering parameters r_H have been considered, using Eq. (2). For the open diamonds, no correction of the calculated n_H has been applied and $m^* = 0.23 m_e$. The blue dots and red triangles consider $m^* = 0.25 m_e$ as reported in the literature[14] as well as Hall scattering factors for ionized impurity (II) scattering and electron-phonon (EP) interaction, respectively. Scattering parameters of $r = -0.5$ and $r = 1.5$ are expected for EP and II interaction, respectively.

© Author(s) 2019

carrier densities, as well as various Hall scattering factors and effective masses for the 185 nm thick high mobility β-Ga_2O_3 thin film.

For r_H = 1 and m^* = 0.23m_e (open diamonds), no correction of the charge carrier density has been done and the effective mass has been used as obtained from temperature dependent charge carrier densities fits. If we consider Hall scattering factors[32] of r_H = 1.93 and r_H = 1.18 for ionized impurity scattering and electron-phonon interaction, respectively, and assume an effective mass of m^* = 0.25m_e as reported in the literature,[14] we obtain the blue dots and red squares for II and EP scattering, respectively. The obtained results near room temperature are in agreement with the expected value of r = −0.5 for electron-phonon-scattering (Fig. 4, lower dashed line).[29,31,32] For β-Ga_2O_3 thin films, electron-phonon-scattering is expected to be the dominant scattering mechanism at these temperatures.[6] Here, the scattering mechanism dominating the charge transfer caused by electrical potential gradients is the same as caused by temperature differences.

For low temperatures, we obtain values close to $r = 3/2$ as expected for ionized-impurity scattering (upper dashed line). This is also in agreement with values reported in the literature.[29,31,32] Ionized impurity scattering has been reported[6,33] to become the dominant scattering mechanism in β-Ga_2O_3 below 100 K, depending on layer thickness and doping. This explains why we obtain values close to 1.5 if we assume that the charge carrier scattering mechanisms influencing the mobility and the Seebeck effect are the same.

The Seebeck coefficients in β-Ga_2O_3 thin films at room temperature are mainly dependent on the doping level since electron phonon scattering is the dominant scattering mechanism, whereas at low temperatures the different dominant scattering mechanisms have a major impact on the magnitude of the Seebeck coefficient. These observations are consistent with previous studies on thermal[8,9] and electrical[6,7] conductivity where the dominant scattering mechanisms at room temperature are phonon-based. For applications at higher temperatures, the room temperature magnitude of the Seebeck coefficient gives an upper limit. Furthermore we can estimate that S approaches a value of $2k_B/e$ in the intrinsic regime.

In conclusion, the temperature dependent Seebeck coefficient of homoepitaxial β-Ga_2O_3 thin films can be explained by the Stratton formula. β-Ga_2O_3 thin films have Seebeck coefficients relative to aluminum of $S_{\beta\text{-}Ga_2O_3\text{-}Al}$ = (−300 ± 20) μV/K at room temperature with an increase in magnitude at lower temperatures. This leads to a room temperature Peltier coefficient of $\Pi \approx 0.1$ V. The dependency of the Seebeck coefficient on the dominant scattering mechanism gives the possibility of Seebeck coefficient engineering by growing β-Ga_2O_3 thin films with, for example, an increased concentration of neutral impurities or ionized impurities.

See supplementary material for details of the two contact configurations investigated.

This work was performed in the framework of GraFOx, partially funded by the Leibniz Association and by the German Science Foundation (Grant Nos. DFG-FI932/10-1 and DFG-FI932/11-1). The authors thank M. Kockert for fruitful scientific discussions.

REFERENCES

[1]S. I. Stepanov, V. I. Nikolaev, V. E. Bougrov, and A. E. Romanov, "Gallium oxide: Properties and application–A review," Rev. Adv. Mater. Sci. **44**, 63–86 (2016).

[2]N. Suzuki, S. Ohira, M. Tanaka, T. Sugawara, K. Nakajima, and T. Shishido, "Fabrication and characterization of transparent conductive Sn-doped β-Ga_2O_3 single crystal," Phys. Status Solidi C **4**, 2310–2313 (2007).

[3]A. J. Green, K. D. Chabak, E. R. Heller, R. C. Fitch, M. Baldini, A. Fiedler, K. Irmscher, G. Wagner, Z. Galazka, S. E. Tetlak, A. Crespo, K. Leedy, and G. H. Jessen, "3.8-MV/cm breakdown strength of MOVPE-grown Sn-doped β-Ga_2O_3 mosfets," IEEE Electron Device Lett. **37**, 902–905 (2016).

[4]K. D. Chabak, N. Moser, A. J. Green, D. E. Walker, S. E. Tetlak, E. Heller, A. Crespo, R. Fitch, J. P. McCandless, K. Leedy, M. Baldini, G. Wagner, Z. Galazka, X. Li, and G. Jessen, "Enhancement-mode Ga_2O_3 wrap-gate fin field-effect transistors on native (100) β-Ga_2O_3 substrate with high breakdown voltage," Appl. Phys. Lett. **109**, 213501 (2016).

[5]Z. Galazka, "β-Ga_2O_3 for wide-bandgap electronics and optoelectronics," Semicond. Sci. Technol. **33**, 113001 (2018).

[6]R. Ahrling, J. Boy, M. Handwerg, O. Chiatti, R. Mitdank, G. Wagner, Z. Galazka, and S. F. Fischer, "Transport properties and finite size effects in β-Ga_2O_3 thin films," e-print arXiv:1808.00308v3.

[7]R. Mitdank, S. Dusari, C. Bülow, M. Albrecht, Z. Galazka, and S. F. Fischer, "Temperature-dependent electrical characterization of exfoliated β-Ga_2O_3 micro flakes," Phys. Status Solidi A **211**, 543–549 (2014).

[8]M. Handwerg, R. Mitdank, Z. Galazka, and S. F. Fischer, "Temperature-dependent thermal conductivity in Mg-doped and undoped β-Ga_2O_3 bulk crystals," Semicond. Sci. Technol. **30**, 024006 (2015).

[9]M. Handwerg, R. Mitdank, Z. Galazka, and S. F. Fischer, "Temperature-dependent thermal conductivity and diffusivity of a Mg-doped insulating β-Ga_2O_3 single crystal along [100], [010] and [001]," Semicond. Sci. Technol. **31**, 125006 (2016).

[10]H. H. Tippins, "Optical absorption and photoconductivity in the band edge of β-Ga_2O_3," Phys. Rev. **140**, A 316–A 319 (1965).

[11]M. R. Lorenz, J. F. Woods, and R. J. Gambino, "Some electrical properties of the semiconductor β-Ga_2O_3," J. Phys. Chem. Solids **28**, 403–404 (1967).

[12]M. Orita, H. Ohta, M. Hirano, and H. Hosono, "Deep-ultraviolet transparent conductive β-Ga_2O_3," Appl. Phys. Lett. **77**, 4166–4168 (2000).

[13]H. Peelaers and C. G. V. de Walle, "Lack of quantum confinement in Ga_2O_3 nanolayers," Phys. Rev. B **96**, 081409 (2017).

[14]C. Janowitz, V. Scherer, M. Mohamed, A. Krapf, H. Dwelk, R. Manzke, Z. Galazka, R. Uecker, K. Irmscher, R. Fornari, M. Michling, D. Schmeißer, J. R. Weber, J. B. Varley, and C. G. V. de Walle, "Experimental electronic structure of In_2O_3 and Ga_2O_3," New J. Phys. **13**, 085014 (2011).

[15]Y. Kang, K. Krishnaswamy, H. Peelaers, and C. G. V. de Walle, "Fundamental limits on the electron mobility of β-Ga_2O_3," J. Phys.: Condens. Matter **29**, 234001 (2017).

[16]M. Mohamed, I. Unger, C. Janowitz, R. Manzke, Z. Galazka, R. Uecker, and R. Fornari, "The surface band structure of β-Ga_2O_3," J. Phys.: Conf. Ser. **286**, 012027 (2011).

[17]Z. Galazka, K. Irmscher, R. Uecker, R. Bertram, M. Pietsch, A. Kwasniewski, M. Naumann, T. Schulz, R. Schewski, D. Klimm, and M. Bickermann, "On the bulk β-Ga_2O_3 single crystal grown by the Czochralski method," J. Cryst. Growth **404**, 184–191 (2014).

[18]R. Stratton, "Diffusion of hot and cold electrons in semiconductor barriers," Phys. Rev. **126**, 2002–2014 (1962).

[19]Z. Galazka, R. Uecker, D. Klimm, K. Irmscher, M. Naumann, M. Pietsch, A. Kwasniewski, R. Bertram, S. Ganschow, and M. Bickermann, "Scaling-up

© Author(s) 2019

of bulk β-Ga_2O_3 single crystals by the Czochralski method," ECS J. Solid State Sci. Technol. **6**, Q3007–Q3011 (2016).
[20]Z. Galazka, R. Uecker, K. Irmscher, M. Albrecht, D. Klimm, M. Pietsch, M. Brützam, R. Bertram, S. Ganschow, and R. Fornari, "Czochralski growth and characterization of β-Ga_2O_3 single crystals," Cryst. Res. Technol. **45**, 1229–1236 (2010).
[21]M. Baldini, Z. Galazka, and G. Wagner, "Recent progress in the growth of β-Ga_2O_3 for power electronics applications," Mater. Sci. Semicond. Process. **78**, 132–146 (2018).
[22]A. Fiedler, R. Schewski, M. Baldini, Z. Galazka, G. Wagner, M. Albrecht, and K. Irmscher, "Influence of incoherent twin boundaries on the electrical properties of β-Ga_2O_3 layers homoepitaxially grown by metal-organic vapor phase epitaxy," J. Appl. Phys. **122**, 165701 (2017).
[23]R. Schewski, K. Lion, A. Fiedler, C. Wouters, A. Popp, S. V. Levchenko, T. Schulz, M. Schmidbauer, S. B. Anooz, R. Grüneberg, Z. Galazka, G. Wagner, K. Irmscher, M. Scheffler, C. Draxl, and M. Albrecht, "Step-flow growth in homoepitaxy of β-Ga_2O_3 (100)-the influence of the miscut direction and faceting," APL Mater. **7**, 022515 (2019).
[24]T. M. Tritt, *Thermal Conductivity: Theory, Properties, and Applications* (Springer, NY, 2004).
[25]A. Z. Barasheed, S. R. S. Kumar, and H. N. Alshareef, "Temperature dependent thermoelectric properties of chemically derived gallium zinc oxide thin films," J. Mater. Chem. C **1**, 4122 (2013).
[26]O. Bierwagen, "Indium oxide—A transparent, wide-band gap semiconductor for (opto)electronic applications," Semicond. Sci. Technol. **30**, 024001 (2015).
[27]D. L. Young, T. J. Coutts, V. I. Kaydanov, A. S. Gilmore, and W. P. Mulligan, "Direct measurement of density-of-states effective mass and scattering parameter in transparent conducting oxides using second-order transport phenomena," J. Vac. Sci. Technol., A **18**, 2978 (2000).
[28]C. Herring, "Theory of the thermoelectric power of semiconductors," Phys. Rev. **96**, 1163–1187 (1954).
[29]D. S. Ginley, *Handbook of Transparent Conductors*, edited by H. Hosono and D. C. Paine (Springer, NY, 2010).
[30]N. G. Nilsson, "An accurate approximation of the generalized Einstein relation for degenerate semiconductors," Phys. Status Solidi A **19**, K75–K78 (1973).
[31]N. Preissler, O. Bierwagen, A. T. Ramu, and J. S. Speck, "Electrical transport, electrothermal transport, and effective electron mass in single-crystalline In_2O_3 films," Phys. Rev. B **88**, 085305 (2013).
[32]S. M. Sze and K. K. Ng, *Physics of Semiconductor Devices* (Wiley-Interscience, 2007).
[33]T. Oishi, Y. Koga, K. Harada, and M. Kasu, "High-mobility β-Ga_2O_3 ($\bar{2}01$) single crystals grown by edge-defined film-fed growth method and their Schottky barrier diodes with Ni contact," Appl. Phys. Exp. **8**, 031101 (2015).

© Author(s) 2019